Talanta 88 (2012) 631–637

Contents lists available at SciVerse ScienceDirect

Talanta

journal homepage: www.elsevier.com/locate/talanta

Real-time monitoring of anticancer drug release *in vitro* and *in vivo* on titania nanoparticles triggered by external glutathione

Mira Kim [a], Ji Hye Seo [a], Won Il Jeon [b], Mi-Yeon Kim [c], Keunchang Cho [d], So Yeong Lee [b,*], Sang-Woo Joo [a,*]

[a] Department of Chemistry, Soongsil University, Seoul 156-743, Republic of Korea
[b] Laboratory of Veterinary Pharmacology, College of Veterinary Medicine and Research Institute for Veterinary Science, Seoul National University, Seoul 151-742, Republic of Korea
[c] School of Systems and Biomedical Science, Soongsil University, Seoul 156-743, Republic of Korea
[d] Logos Biosystems, Inc., Anyang 431-070, Republic of Korea

ARTICLE INFO

Article history:
Received 15 September 2011
Received in revised form
16 November 2011
Accepted 17 November 2011
Available online 25 November 2011

Keywords:
Real-time monitoring
Drug release
Nanoparticles
Glutathione
Live cell imaging

ABSTRACT

The anticancer drug doxorubicin (DOX) appeared to adsorb efficiently on TiO_2 nanoparticles (NPs) as evidenced by visible absorption and diffuse reflectance infrared spectroscopy data. The adsorbed drugs were found released in a controlled way by external glutathione (GSH). Fluorescence of DOX appeared to be quenched substantially by TiO_2 NPs. The fabrication and release of DOX on TiO_2 NPs were checked by monitoring the fluorescence. We could monitor real-time drug release in the live cell using fluorescence imaging techniques. By these methods, we were able to monitor up to a nanomolar amount of DOX release *in vitro* from TiO_2 NPs triggered by external GSH. *In vivo* fluorescence images of DOX were obtained from the subcutaneous site in living mice after GSH treatment. On the basis of label-free fluorescence quenching measurements, a real-time release of DOX on TiO_2 NPs can be monitored *in vitro* and *in vivo* after an external trigger of GSH.

1. Introduction

Nanostructured materials are used in a wide variety of applications including sensors, targeted drug delivery, therapeutic agents, cellular imaging and diagnostics [1]. Nanoparticles have been used to detect a trace amount of analyte using spectroscopic tools [2]. Drug delivery systems provide important tools for enhancing the efficacy of chemotherapeutics [3]. TiO_2-based materials have been recently introduced in detection dyes [4] and drug delivery systems [5–7].

For many practical drug delivery applications, stimuli-responsive release of the pharmaceutical cargo should improve the therapeutic efficacy [8–10]. Although numerous drug encapsulations have been developed, the release of the drugs in a controlled manner remains a challenge after the drug molecules' cellular internalization. There have been several reports on the pH-triggered [11] and photo-induced drug release [12]. Externally triggered glutathione (GSH) has been utilized to release the drug molecules [13].

It is crucial to monitor intracellular controlled drug release by means of external stimulus in real time. Live-cell imaging is one of the most effective techniques for noninvasive and real-time studies of the dynamic interactions in living cells [14]. Due to its strong fluorescence and surface accessibility of the OH groups, doxorubicin (DOX) has been widely used in anticancer drug imaging. The biomolecule such as dopamine are known to adsorb on TiO_2 surfaces via its OH groups [15]. Since NPs can quench fluorescence effectively, they have been employed in biomolecular imaging or ultrasensitive sensing [16].

This work was motivated because there are quite limited label-free spectroscopic studies on the drug release inside live cells in real time without using additional fluorescence dyes. Fluorescence appeared to be quenched on TiO_2 surfaces. In this work, we report intracellular drug release monitoring in the live cell using fluorescence imaging techniques. By these methods, we are able monitor up to a nanomolar amount of doxorubicin release from TiO_2 NPs triggered by GSH. *In vivo* fluorescence images of doxorubicin were also obtained from the subcutaneous site in living mice after GSH treatment.

2. Experimental

2.1. Materials

TiO_2 NPs were purchased from Ovonik. A 50 mg quantity of P-25 TiO_2 was added to 50 mL of ethanol, and the suspension was sonicated for 30 min. Doxorubicin (DOX) hydrochloride (Adriamycin)

* Corresponding authors. Tel.: +82 2 8801283; fax: +82 2 8200434.
E-mail addresses: leeso@snu.ac.kr (S.Y. Lee), sjoo@ssu.ac.kr (S.-W. Joo).

0039-9140/$ – see front matter © 2011 Elsevier B.V. All rights reserved.
doi:10.1016/j.talanta.2011.11.049

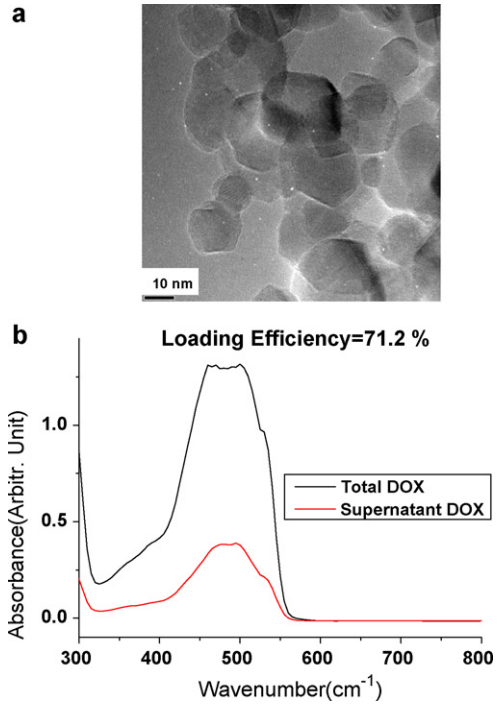

Fig. 1. (a) TEM image of TiO_2 NPs. (b) Loading efficiency of DOX from the decrease in the absorbance measurements. The concentrations of DOX and TiO_2 NPs are 9.1×10^{-5} M and 80 ppm, respectively.

was purchased from Selleck chemicals. GSH, GSH-OEt, and GSH assay kit were purchased from Sigma Aldrich. LysoTracker Blue was purchased from Invitrogen.

2.2. Physicochemical characterization

The transmission electron microscopy (TEM) images were obtained using a JEOL JEM-1010 microscope at an acceleration voltage of 40–100 kV. UV–vis absorbance spectrum of the TiO_2 NP solution was taken using a Mecasys 3220 spectrophotometer. The dynamic light scattering (DLS) measurements were used to estimate the hydrodynamic radius of the TiO_2 NPs particles with an Otsuka ELSZ-2 analyzer. The crystalline structures of the TiO_2 NPs were examined by X-ray diffraction (XRD) patterns observed by Rigaku Miniflex X-ray diffractometer. The fabrication of DOX on TiO_2 NPs via self-assembly was checked by diffuse reflectance infrared spectroscopic tools at 64 scans with a resolution of 4 cm^{-1} using a Thermo 6700 Fourier-transform infrared spectrometer. A portion of the DOX-assembled TiO_2 NP sample was transferred onto a DiffuseIR chamber (Pike Technologies) [17]. Fluorescence spectra were obtained using a Scinco FS-2 spectrometer. Loading efficiency is estimated to the following formula as recently report [18].

$$\text{Loading efficiency}\,(\%) = \left[\frac{\text{total amount of DOX added} - \text{amount of DOX in supernatant}}{\text{total amount of DOX added}}\right] \times 100.$$

2.3. Cell culture

Human lung carcinoma A549 cancer cells were tested to check their viability after the cellular uptake of the TiO_2 NPs. A549 cells were grown on RPMI in a steri-cycle CO_2 incubator (Thermo Fisher Scientific). All cells were supplemented with 10% fetal bovine serum and 1% penicillin-streptomycin antibiotics (Gibco)/0.2 ppm plasmocin and maintained in 5% CO_2/95% humidified air at 37 °C. Approximately 10^5–10^6 cells were washed with phosphate buffer saline and 0.25% trypsin-EDTA was added for 3 min to detach the cells and counted by a hematocytometer. Dulbecco's phosphate buffered saline (DPBS) was used to wash seeded cells. After adding 1 mL of trypsin solution, the cells were incubated at 37 °C for 3 min and then 5 mL of the medium solution was added subsequently. Detached cells were transferred into a new culture dish and incubated at 37 °C with a 5% CO_2 incubator. A cover glass (Fisher) was embedded into a 100 mm × 20 mm size Petri dish. A 0.2% gelatin was coated onto a cover glass and remained for 30 min at room temperature. After 30 min, a number of 3×10^5 cells were seeded onto a medium of a 10% FBS solution and a 1% antibacterial reagent at 37 °C, 5% CO_2 in an incubator for overnight. A cover glass seeded the cells was placed in a live cell chamber (LCI instrument) at a maintained temperature of 37 °C.

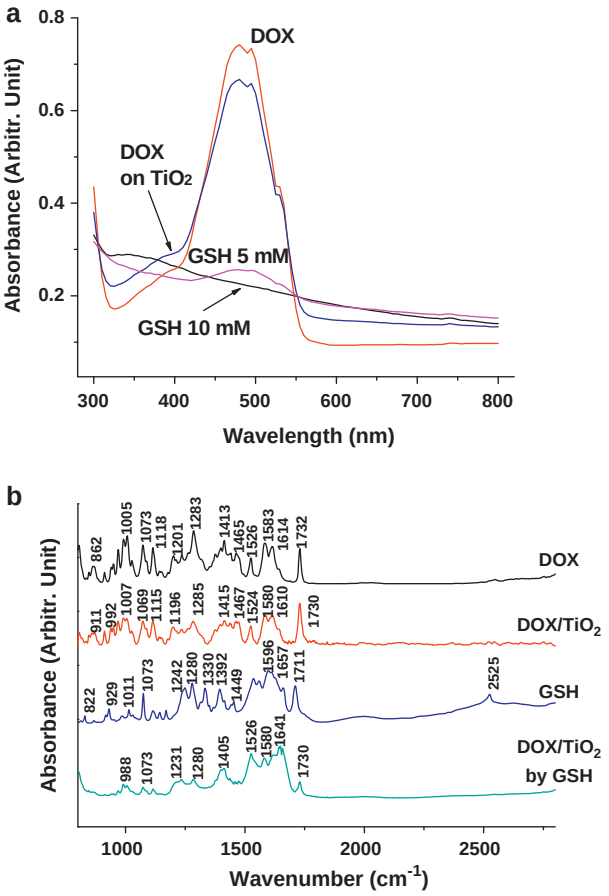

Fig. 2. (a) Absorption and (b) infrared spectra of DOX on TiO_2 NPs before and after treating GSH. UV–vis absorption spectra of DOX and TiO_2 NPs (80 ppm). Desorption of DOX (3×10^{-4} M) by GSH (5 mM and 10 mM).

2.4. Transmission electron microscopy (TEM) of cellular uptake of NPs

The high-resolution images and the uptake of NPs were examined using a JEOL JEM-3010 and a JEM-1010 TEM microscope, respectively. A549 cells were plated on a 100 mm culture dish (SPL, Korea) at a concentration of 5×10^4 cells per dish containing growth medium before the cells were exposed to the NPs. NPs

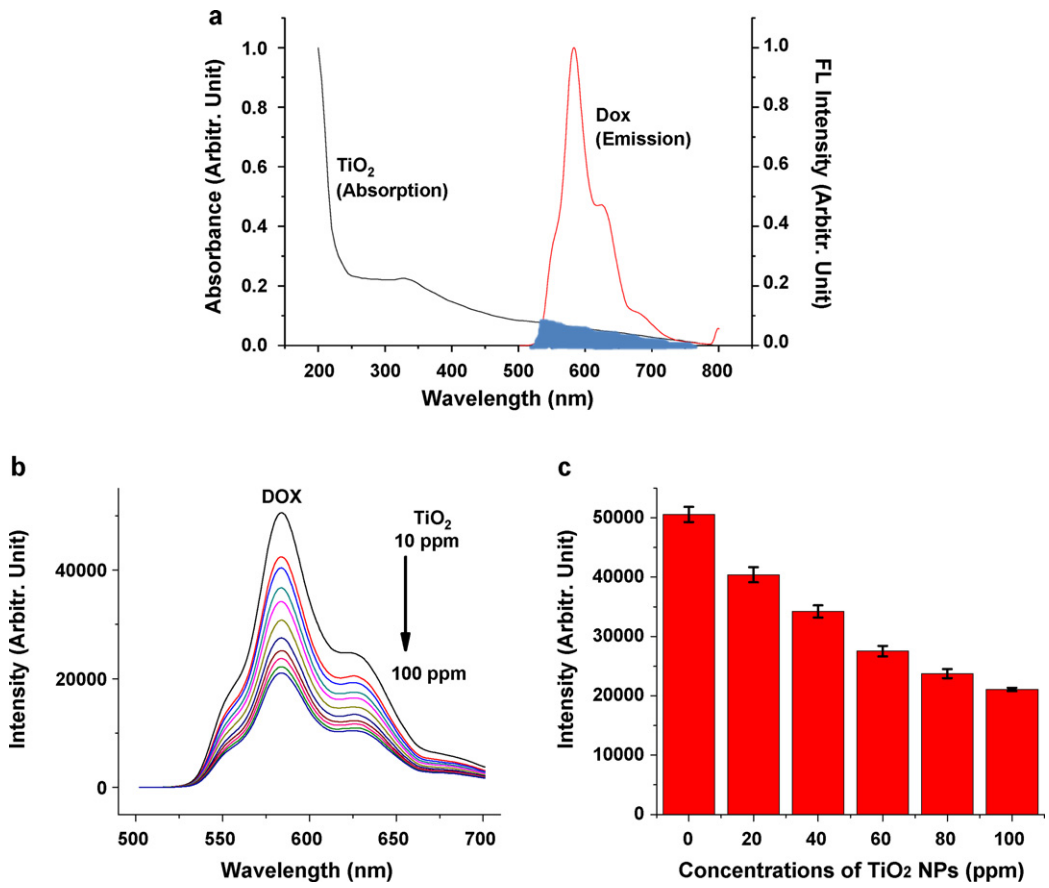

Fig. 3. Quenching of fluorescence in DOX by TiO_2 NPs. (a) Spectrum overlap between the absorption of TiO_2 NPs (80 ppm (μg/mL), black line) and fluorescence emission of DOX in ethanol (3×10^{-4} M, red line). (b) Depending on the concentrations of TiO_2 NPs in the range of 10–100 ppm, fluorescence decreases. The initial volume and concentration of DOX are 1 mL and 3×10^{-3} M, respectively. The volume of added TiO_2 NPs is equally 10 μL for 10–100 ppm samples using a micropipet. The fluorescence was measured 10 min after the mixing the solution. (c) Stick diagram of decrease in fluorescence intensities of DOX. The error bars indicate the standard deviations of the three independent measurements. (For interpretation of the references to color in this figure legend, the reader is referred to the web version of the article.)

were added, and the cells were incubated at 37 °C with 5% CO_2. After 24 h, the cells were washed twice with DPBS, fixed in Karnovsky's fixative for 24 h, and post-fixed in 0.5 M of osmium tetroxide. After fixation, specimens were rinsed with and dehydrated in a graded series of 30, 50, 70, 80, 90% ethanol and three times in 100% ethanol, for 15 min each. Samples were embedded in a mixture of resin in propylene oxide polymerized at 80 °C. Ultrathin sections for TEM were prepared with a diamond knife. Samples were analyzed using a transmission electron microscope.

2.5. Fluorescence images of cellular uptake of NPs

An Olympus IX-71 inverted microscope was employed with a Hg lamp (U-LH100HG) and a high sensitive CCD camera (CoolSnap HQ2, Roper Scientific). An objective lens (40× or 60×) with a corrected thickness for the cover glass was used to obtain the image using the CCD camera. The filter set for DOX consists of 460–490 nm excitation, 506 nm dichroic, and 575 nm emission (Semrock). A shutter (Ludl Electronic Products Ltd.) with a MAC6000 shutter controller was employed to give a 300 ms exposure time by a MetaMorph ID34072 software.

2.6. Cytotoxicity and GSH assay

For cell viability test, a CCK-8 kit purchased from Dojindo was used as received. We applied CCK-8 cytotoxicity assays of DOX and TiO_2 NPs using a 96 well plate (SPL, Korea) and a Tecan Infinite F50 absorbance reader after 24 h incubation of TiO_2 NPs. Intracellular GSH levels were measured using a fluorescence method [19]. We used a fluorescence assay kit (Sigma Catalogue #CS1020) with a Tecan F200 96 well plate reader. The kit assay utilizes a thiol probe (monochlorobimane), which can freely pass through the plasma membrane. The free, unbound probe shows very little fluorescence, but when bound to reduced glutathione in a reaction that is catalyzed by glutathione S-transferase (GST) it forms a strongly fluorescent adduct. The microplate was then incubated at room temperature before being measured at an excitation/emission of 360/485 nm using a fluorescent plate reader. Estimation of protein was done using a bicinchoninic acid (BCA) protein assay kit (Intron Biotechnology Catalogue # 21071) for the colorimetric detection and quantification of total protein using a Tecan F50 microplate reader.

2.7. In vivo imaging

The fluorescence emission profiles of DOX in living mice were obtained using a fully automated CRi Maestro™ 2 *in vivo* imaging system at the wavelength between 500 and 800 nm using a Xenon illuminator. Six week old male CAnN.Cg-Foxn1nu/CrljOri nude mice (Orient Bio Inc, Gyeonggi, Korea) were used for *in vivo* fluorescence measurements. Quantitative information out of the samples could be obtained using a Maestro imaging software.

3. Results and discussion

3.1. Physical characterization and fabrication of DOX on TiO_2 NPs via self-assembly

Fig. 1(a) shows the high-resolution TEM image of TiO_2 NPs. The transmission electron microscopy (TEM) images of DOX-assembled TiO_2 NPs exhibited an average diameter of ~50 nm. The fabrication of DOX appeared to occur on TiO_2 NPs via self-assembly. The loading efficiency of DOX on TiO_2 NPs could be estimated by absorbance measurements after the separation of the unbound supernatant DOX from the adsorbed one on TiO_2.

3.2. Release of DOX on TiO_2 NPs via GSH

The adsorption of DOX on TiO_2 was further checked by absorption and diffuse reflectance infrared spectroscopic tools. The absorption spectra of DOX maximized at 480 nm indicated the attachment of DOX on TiO_2 as shown in Fig. 2(a). We could observe more displacement at higher concentration of GSH in the range between 5 and 20 mM. The infrared bands at 1614 and 1583 cm^{-1} can be assigned to the ring modes [20] of DOX as shown in Fig. 2(b). The chemical interaction of DOX on TiO_2 was presumed to occur via their OH group. It has been reported that anthracyclin anticancer drugs such as DOX and daunorubicin can adsorb on carbon materials via π–π interactions [22,23]. Due to the multicrystalline structure, it is likely that DOX adsorb on of TiO_2 NPs via either covalent bonding or van der Walls interactions.

These bonds were found to be replaced by GSH. As shown in Fig. 2(a) and (b), the SH band 2525 cm^{-1} of GSH disappeared upon adsorption on TiO_2 NP, which indicates a stronger adsorption of GSH than the drug molecule. It was found that the DOX peaks at 1730 and 1405 cm^{-1} still remained to indicate that there should be the remnants of DOX on TiO_2 even after the GSH treatment. As shown in Fig. 2(a) and (b), GSH appeared to replace DOX from the infrared and absorption spectra, respectively. After GSH was treated to the DOX-assembled TiO_2 NP, the vibrational structures of DOX showed a considerable decrease with the appearance of those of GSH. The absorption spectra of DOX maximized at 480 nm also almost disappeared due to the detachment of DOX by GSH. As shown in Fig. 2(a) and (b), DOX was replaced by GSH. We used the GSH amount to consider the intracellular conditions 1–10 mM. We also used a tripeptide containing the methyl group instead of a thiol group with a similar molecular weight to GSH not to observe the release of drug molecules on NPs. We concluded that the reducing capability of the thiol group should lead to the desorption of the adsorbates on NPs.

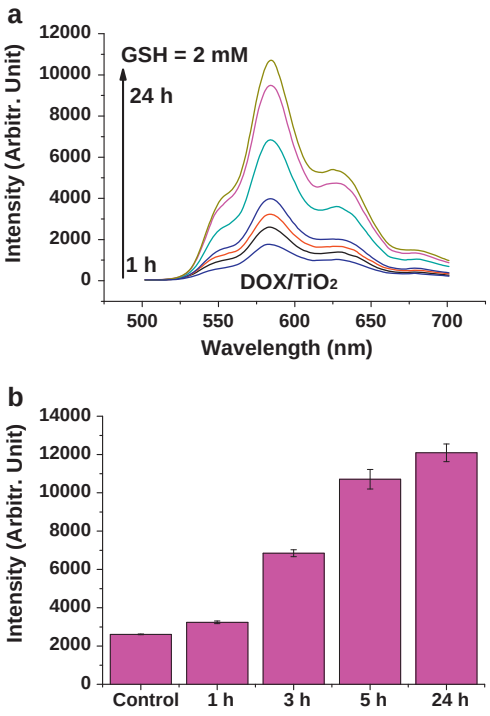

Fig. 4. (a) Plot of time-dependent fluorescence intensities by treating GSH (2 mM). The concentrations of DOX and TiO_2 NPs are 5.0×10^{-5} M and 80 ppm, respectively. (b) Stick diagram. The error bars indicate the standard deviations of the three independent measurements.

3.3. Fluorescence quenching of DOX on TiO_2 NPs

Fluorescence of DOX appeared to be quenched by TiO_2 NPs. Due to the decrease of quenching effects from TiO_2 NPs, the desorption of DOX replaced by GSH increased the fluorescence. Fig. 3(a) shows the spectrum overlap (blue color) between the DOX's fluorescence emission and the absorption of TiO_2 NPs. DOX has its own fluorescence emission maximum at 580 nm. It is found that TiO_2 particles can quench the fluorescence of DOX. As the concentrations of DOX increase in the range from 10 to 100 ppm (μg/mL), the fluorescence signals dropped accordingly. UV–vis spectra of TiO_2 NPs

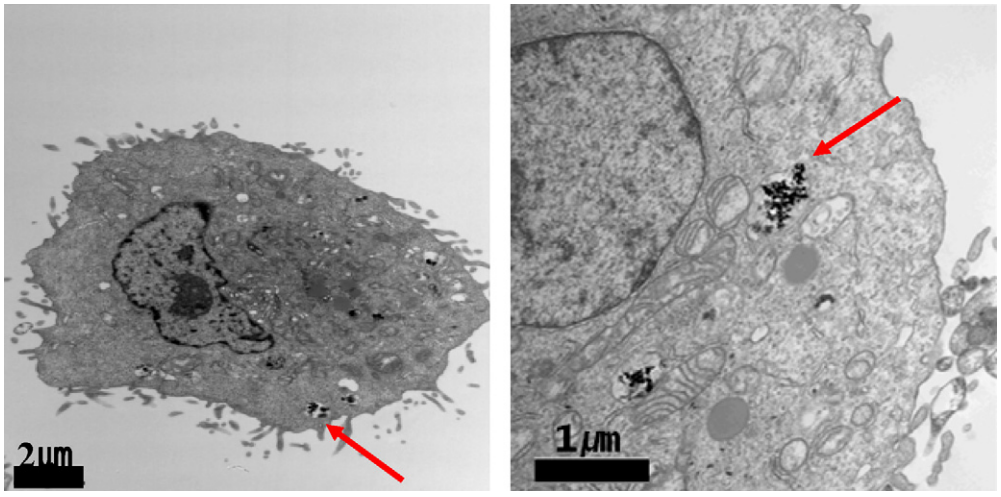

Fig. 5. TEM image of DOX-assembled TiO_2 NPs in A549 cells. The arrows indicate the locations of intracellular TiO_2 NPs.

Table 1
Diameters, size increase after adsorption of DOX and decrease by serum proteins on TiO_2 NPs.

Hydrodynamic diameter (nm)[a]	Diameters after adsorption of DOX (9.1×10^{-5} M)[b] (nm)[a]	Diameters after adsorption of RPMI with 10% FBS (nm)[a]
136.4 ± 10.6	283.6 ± 25.2	80.0 ± 3.4

[a] The sizes are based on the DLS measurements.
[b] The concentration of DOX.

showed a substantial light absorption in the wavelength region of the DOX emission. It was found that the fluorescence was not completely quenched under our experimental conditions. Fig. 4(a) and (b) shows that the fluorescence spectra of DOX increased as time elapsed. We could observe more difference from 3 to 24 h, whereas the data in Fig. 3 were measured only after 10 min. Based on the recent study of the quenching of fluorescent molecules upon the adsorption on NPs, a static quenching mechanism would be efficient instead of dynamic or collisional quenching [24]. The binding constant of DOX on TiO_2 NPs was estimated to be 1.285×10^8 M^{-1} using Stern–Volmer plot.

3.4. Uptake of DOX-assembled TiO_2 NPs in mammalian cells

In the TEM images of A549 cells, we could observe the particle load as an aggregated form inside the cells as shown in Fig. 5. From the ICP-MS measurements, the Ti content was 1.299 ppm for the A549 cell (34.1 mg) with TiO_2 NP solution (80 μg). Considering the

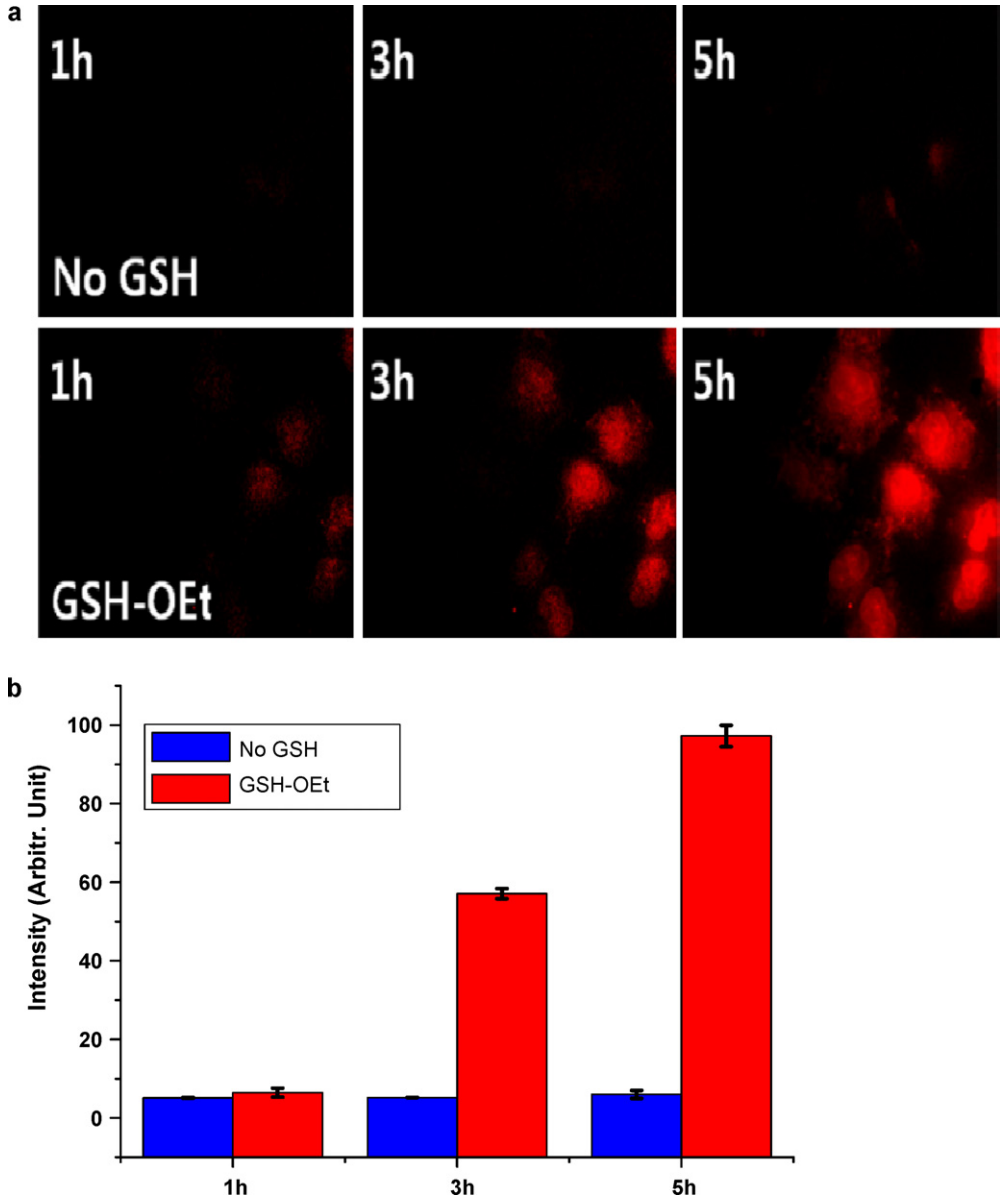

Fig. 6. (a) Fluorescence images of DOX (4 nM) assembled on TiO_2 NPs (8 ppm (μg/mL)) by using GSH-OEt (>5 mM) as an external stimulus in A549 cells for 1–5 h. Upper: control, lower: GSH-OEt. DOX-assembled TiO_2 NPs were incubated for 5 h for the initial uptake. The upper and lower pictures are the fluorescence images without and with GSH-OEt. (b) Stick diagram for the intensities measured by flow cytometry.

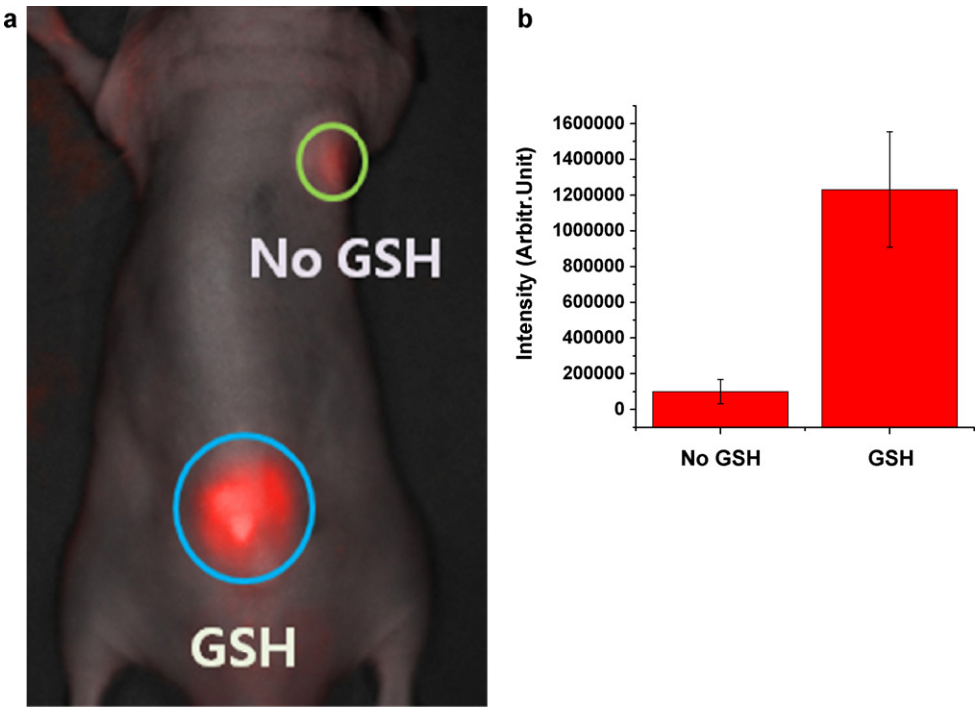

Fig. 7. (a) *In vivo* release of DOX with or without treatment of GSH. A volume of 50 μL of DOX (2×10^{-4} M)-assembled TiO_2 NPs was subcutaneously injected to mice. A volume of 16 μL of GSH was subsequently applied to the same spot with the resulting concentration of ~5 mM within 5 min from the injection of DOX-assembled TiO_2 NPs. We checked that the fluorescence changes were not affected by the injected sites by switching the positions. The injected sites are marked with circles. The fluorescence intensities are measured within 30 min from the sample injection. (b) Stick diagram of the fluorescence recovery of DOX by GSH. The error bars indicate the standard deviations of the three independent measurements.

initial mass of the cells and treated TiO_2 NP solution, the uptake percentage was estimated to be around 0.05%. As summarized in Table 1, DLS data indicate that the NPs increased by assembly of DOX appeared to be subsequently stabilized by the cell culture medium due to the interactions with proteins or lipids. The intracellular aggregation of TiO_2 NPs is presumed to occur after receptor mediated endocytosis. The entrapment of TiO_2 NPs in an endosomal or a lysosomal structure supported that TiO_2 NPs should enter the cell and become accumulated after the coating of the proteins in the cell culture media. Although now shown here, a colocalization image of DOX-assembled TiO_2 NPs in cells and lysosome which indicates a partial overlap. We performed the inhibition test of the cellular uptake by treating chlorpromazine and genistein. Under our experimental conditions, genistein is more effective at blocking the uptake to indicate the caveolae-mediated endocytosis, although this finding is not definite. Since that the uptake was reduced below ~40% at 4 °C, the receptor-mediated endocytosis should be the uptake mechanism [25].

3.5. Cytotoxicity of DOX-assembled TiO_2

For the safe and practical usages of DOX-assembled TiO_2 NPs, cytotoxicity was tested using a CCK-8 analysis. The TiO_2 NPs (8 ppm (μg/mL)) did not appear to affect the cell's viability significantly. Fluorescence images of DAPI-stained A549 cells taken in order to label nuclei activity suggest that the nuclei damage by DOX. It was found that A549 cells, particularly for the nuclei, are substantially damaged by the treatment of TiO_2 NPs. With the concentration of TiO_2 NPs (90 ppm (μg/mL)), a majority of the cancer cells (>60%) were killed, whereas the sole use of DOX could damage the cells effectively above 70 nM, although the data are not shown here. This result is in agreement with the report that there was a significant increase in oxidative stress at higher TiO_2 nanoparticle concentrations (>60 ppm (μg/mL)) [21]. After checking that the toxicity of used TiO_2 NPs (8 ppm) was fairly low from the cell viability test, we performed GSH-triggered DOX release (4 nM) from NPs *in vitro*. The TiO_2 NPs used in the experiment did not show much cytotoxicity from the cell viability test at low concentrations however. To further extend the GSH-triggered drug release, we performed an *in vivo* experiment. DOX-assembled NPs were administered via subcutaneous injection.

3.6. Live cell imaging of DOX-assembled TiO_2 NPs in mammalian cells

Based on these data, we performed a real-time fluorescence live cell imaging experiment in the presence of externally supplied GSH. DOX-assembled TiO_2 NPs were found well internalized in mammalian cancer cells. Fluorescence of DOX quenched by TiO_2 NPs appeared to increase when GSH was externally supplied *in vitro*. Although not shown here, the intracellular GSH levels appeared to increase by 20–80% by treating GSH-OEt (5–20 mM).

Intracellular GSH-triggered release of DOX on TiO_2 NPs was directly monitored using a label-free fluorescence live cell imaging technique in live human carcinoma cells. In our live cell imaging data, highly concentrated DOX (2×10^{-4} M)-assembled TiO_2 NPs (80 ppm (μg/mL)) could enter the cell within an hour. As shown in Fig. 6(a) and (b), the quenched fluorescence appeared to be recovered by glutathione monoester (GSH-OEt), which was used instead of anionic form of GSH in solution due to its inefficient penetration into the cellular membranes [13]. For the live cell imaging data in Fig. 6(a), we used relatively low concentrations of TiO_2 NPs and DOX to observe the GSH-triggered release.

3.7. In vivo imaging of DOX-assembled TiO_2

As shown in Fig. 7, the total fluorescence intensities increased by a factor of 10 after treating high concentration of GSH (~5 mM).

The release of DOX appears to increase by an order of magnitude larger. The GSH concentration in the *in vivo* experiments was higher than that in the *in vitro* experiment in Fig. 4. Our results indicate that DOX-assembled TiO_2 NP systems can be utilized as an effective controlled drug release platform both *in vitro and in vivo*.

4. Conclusion

We found that DOX could adsorb on TiO_2 NP surfaces via self-assembly. The adsorbed DOX appeared to detach from the TiO_2 surfaces after treating GSH (>2 mM). Both *in vitro* and *in vivo* monitoring of DOX could be achieved in real time using TiO_2 NPs as a platform. The amount of the used TiO_2 NPs appeared to show low toxicity from the cell viability test. Our method will be useful to develop a new method of quantifying intracellular drug release in live cells.

Acknowledgements

This work was supported by the Basic Science Research Program through the National Research Foundation of Korea (NRF) funded by the Ministry of Education, Science, and Technology (2011-0001316, 2011-0027696) and the Development of Characterization Techniques for Nano-materials Safety Project of KRCF.

References

[1] X. Michalet, F.F. Pinaud, L.A. Bentolila, J.M. Tsay, S. Doose, J.J. Li, G. Sundaresan, A.M. Wu, S.S. Gambhir, S. Weiss, Science 307 (2005) 538–544.
[2] H. Wang, A.D. Campiglia, Talanta 83 (2010) 233–240.
[3] R. Langer, D.A. Tirrell, Nature 428 (2004) 487–492.
[4] S.S. Mandal, A.J. Bhattacharyya, Talanta 82 (2010) 876–884.
[5] E.A. Rozhkova, I. Ulasov, B. Lai, N.M. Dimitrijevic, M.S. Lesniak, T. Rajh, Nano Lett. 9 (2009) 3337–3342.
[6] M. Song, C. Pan, J. Li, R. Zhang, X. Wang, Z. Gu, Talanta 75 (2008) 1035–1040.
[7] Y.Y. Song, F. Schmidt-Stein, S. Bauer, P.J. Schmuki, J. Am. Chem. Soc. 131 (2009) 4230–4232.
[8] M.S. Muthu, C.V. Rajesh, A. Mishra, S. Singh, Nanomedicine 4 (2009) 657–667.
[9] M. Delcea, H. Möhwald, A.G. Skirtach, Adv. Drug Deliv. Rev. 63 (2011) 730–747.
[10] A.C. De Las Heras, S. Pennadam, C. Alexander, Chem. Soc. Rev. 34 (2005) 276–285.
[11] S. Aryal, J.J. Grailer, S. Pilla, D.A. Steeber, S. Gong, J. Mater. Chem. 19 (2009) 7879–7884.
[12] S. Ibsen, E. Zahavy, W. Wrasdilo, M. Berns, M. Chan, S. Esener, Pharm. Res. 27 (2010) 1848–1860.
[13] R. Hong, G. Han, J.M. Fernández, B.J. Kim, N.S. Forbes, V.M. Rotello, J. Am. Chem. Soc. 128 (2006) 1078–1079.
[14] J.H. Seo, K. Cho, S.Y. Lee, S.-W. Joo, Nanotechnology 22 (2011) 235101.
[15] K. Syres, A. Thomas, F. Bondino, M. Malvestuto, M. Grätzel, Langmuir 26 (2010) 14548–14555.
[16] G.-X. Liang, H.-Y. Liu, J.-R. Zhang, J.-J. Zhu, Talanta 80 (2010) 2172–2176.
[17] Y.M. Jung, Y. Park, S. Sarker, J.-J. Lee, S.-W. Joo, Sol. Energy Sol. Mater. 95 (2011) 326–331.
[18] S. Dhar, E.M. Reddy, A. Prabhune, V. Pokharkar, A. Shiras, B.L.V. Prasad, Nanoscale 3 (2011) 575–580.
[19] M.J. Clift, M.S. Boyles, D.M. Brown, V. Stone, Nanotoxicology 4 (2010) 139–149.
[20] G. Das, A. Nicastri, M.L. Coluccio, F. Gentile, P. Candeloro, G. Cojoc, C. Liberale, F. De Angelis, E. Di Fabrizio, Micros. Res. Tech. 73 (2010) 991–995.
[21] C.Y. Jin, B.S. Zhu, X.F. Wang, Q.H. Lu, Chem. Res. Toxicol. 21 (2008) 1871–1877.
[22] Z. Liu, X. Sun, N. Nakayama-Ratchford, H. Dai, ACS Nano 1 (2007) 5–56.
[23] H. Jiang, X.-M. Wang, Electrochem. Commun. 11 (2009) 126–129.
[24] U.H.F. Bunz, V.M. Rotello, Angew. Chem. Int. Ed. 49 (2010) 3268–3279.
[25] J. Rejman, A. Bragonzi, M. Conese, Mol. Ther. 12 (2005) 468–474.